Applied Materials Today 10 (2018) 218–226

Contents lists available at ScienceDirect

Applied Materials Today

journal homepage: www.elsevier.com/locate/apmt

Review

An overview of recent applications of reduced graphene oxide as a basis of electroanalytical sensing platforms

Samuel J. Rowley-Neale[a,b], Edward P. Randviir[a], Ahmed S. Abo Dena[c,d], Craig E. Banks[a,b,*]

[a] Faculty of Science and Engineering, Manchester Metropolitan University, Chester Street, Manchester M1 5GD, UK
[b] Manchester Fuel Cell Innovation Centre, Manchester Metropolitan University, Chester Street, Manchester M1 5GD, UK
[c] National Organization for Drug Control and Research (NODCAR), Giza, Egypt
[d] Faculty of Oral and Dental Medicine, Future University in Egypt (FUE), New Cairo, Egypt

ARTICLE INFO

Article history:
Received 18 April 2017
Received in revised form
16 November 2017
Accepted 18 November 2017

Keywords:
Sensing
Graphene
Reduced graphene oxide
Electrochemical
Detection

ABSTRACT

The academic literature using graphene within the field of electrochemistry is substantial. Graphene can be fabricated via a plethora of routes with each having its own unique merits (e.g. cost, fabrication time, quality and scale) and reduced graphene oxide (rGO) is more often the material of choice for electrochemical sensors and associated applications due to its ease of fabrication and ability to be mass produced on the kilogram scale. This review overviews pertinent developments in the use of rGO as the basis of electroanalytical sensors (2016–2017); guidelines for the progression of this field are also given.

Contents

1. Introduction

Graphene is now extensively researched since the advent of its reported range of physical properties back in 2004 and 2005 [1,2] and it is acknowledged that graphene has been theoretically explored since the 1940s and known to exist since the 1960s [3]. There are a substantial number of papers reporting the use of graphene in the field of electrochemistry making it now impossible to summarise the field in a single review. Consequently in this paper, we focus and only overview the recent field of electroanalytical sensors from 2016 to 2017.

The fabrication of graphene is achieved by a plethora of ways, as identified within Figs. 1 and 2 each of which having their own merits; there are many papers and reviews that focus extensively upon the variety of fabrication methodologies and as such, will not be covered here. Cleary pristine graphene can be fabricated allowing the fundamental understanding of graphene to be deduced but is not readily used as the basis of electrochemical sensors due to its high cost and lack of manufacturing scalability. Other forms of graphene are thus explored, due to these very reasons. As such, reduced graphene oxide (rGO) is widely utilised, which is usually fabricated from the oxidation/exfoliation of graphite to graphene oxide (GO) and then its reduction to graphene via a variety of routes such as chemical, thermal or electrochemical; this is summarised within Fig. 2. There are clearly a wide range of ways to produce graphene, ranging from producing pristine graphene through to what is termed rGO.

Initially, it is pertinent to define exactly what graphene oxide (GO) and rGO is. Dreyer et al. [4] have usefully provided a summary: GO is chemically modified graphene, which is prepared by oxidation and exfoliation that is accompanied by extensive modification of the basal plane. GO is a monolayer with a high oxygen content, typically characterised by a C/O ratio of less than 3:1 and

* Corresponding author at: Faculty of Science and Engineering, Manchester Metropolitan University, Chester Street, Manchester M1 5GD, UK.
E-mail address: c.banks@mmu.ac.uk (C.E. Banks).

https://doi.org/10.1016/j.apmt.2017.11.010

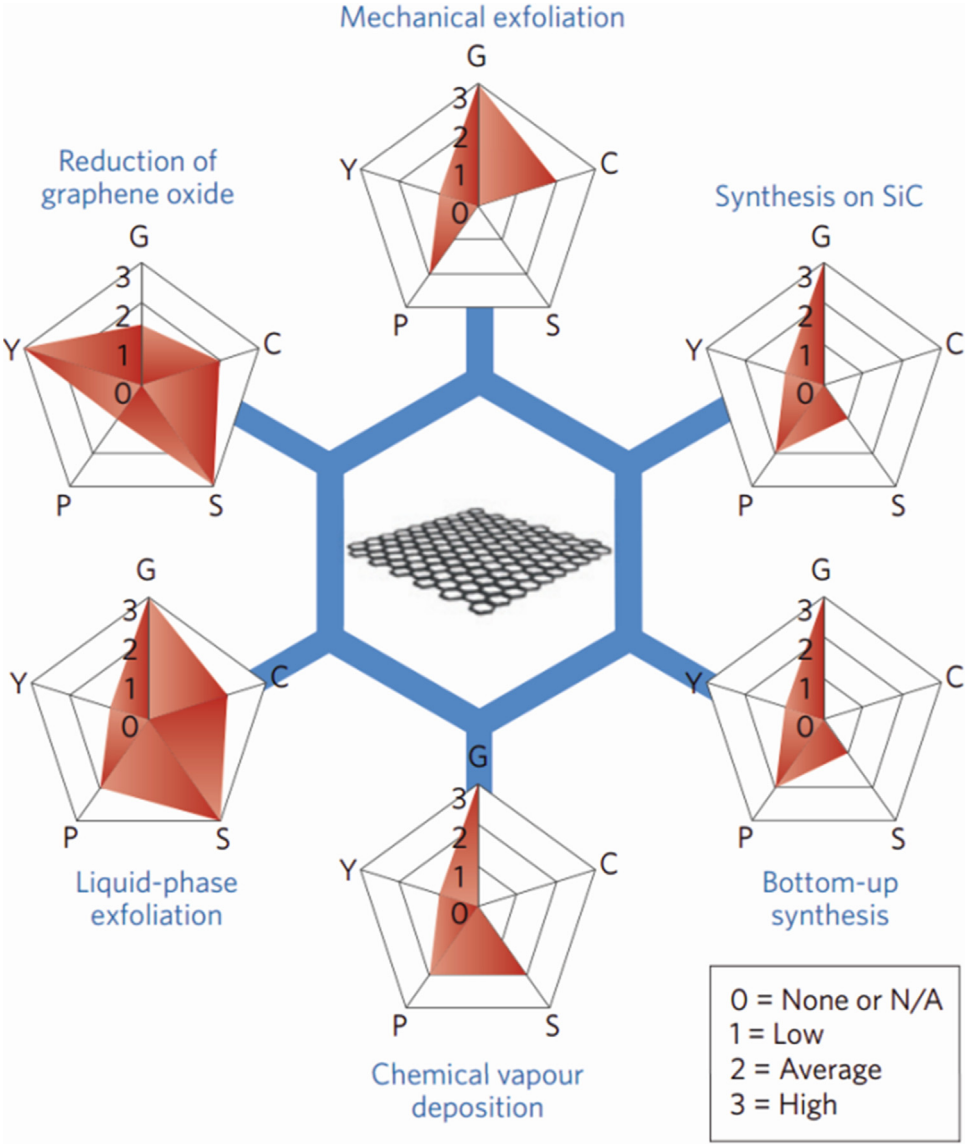

Fig. 1. The most common graphene production methods. Each method has been evaluated in terms of graphene quality (G), cost aspect (C; a low value corresponds to high cost of production), scalability (S), purity (P) and yield (Y) of the overall production process.
Reprinted with permission from Nature [41].

typically closer to 2:1, respectively. Note that GO is not a new material given that it has been known to exist since the 1840s [4–6]. It has been largely overlooked in this field of research, being considered predominately as a precursor for graphene synthesis. Brodie [6] reported that *graphite oxide* is defined as: bulk solid made by the oxidation of graphite through processes that functionalise the basal planes and increase the interlayer spacing. Graphite oxide can be exfoliated in solution to form (monolayer) graphene oxide or partially exfoliated to form few-layer graphene oxide. Thus, rGO is defined (as above) that has been reductively processed by chemical, thermal, microwave, photo-chemical, photo-thermal or microbial/bacterial methods to reduce its oxygen content.

Interestingly, GO is reported to have limited electrical and thermal transport due to the oxygen functionalisation on the basal plane surface [7], and it has been largely overlooked in this field of research, being considered predominantly as a precursor for the synthesis of graphene. GO has been reported to be beneficial in a very few electrochemistry areas [8,9], such as in energy storage devices [10], and nucleic acid monitoring [11]. Recent work by Brownson et al. [12] has demonstrated that GO, used as is, gives rise to unique electrochemical responses where the oxygenated species encompassing GO strongly influence and dominate the observed voltammetry, which is crucially coverage dependant. rGO is an interesting member of the graphene family since it, along with GO, are the only variants where fabrication can be scale-up and be manufactured on the kilogram scale [7]. The fundamental understanding of graphene is generally explored using graphene that is made *via* mechanical exfoliation or Chemical Vapour Deposition (CVD) [13–16], *i.e.* pristine graphene, which allows stricter control over the number of graphene layers, but fundamental work on rGO is yet to be fully explored, although general trends can be readily transferred such as the density of edge plane like – sites/defects/number of graphene layers dominating the electrochemical response [17,18]. Note the C/O ratio is not zero, *i.e.* like pristine graphene and the C/O amount and type of C—O groups may influence its electrochemical response.

In this review, we overview recent developments utilising rGO as the basis of electroanalytical sensors. Table 1 provides an overview summarising the last two years contribution to this field; we limit this timeframe due to the sheer volume of publications.

Table 1
Examples of some of the recent studies that utilise rGO and GO as the basis of electroanalytical sensors.

Analytical target	Supporting electrode/substrate	Catalytic material utilised	Graphene fabrication method	Sensitivity ($\mu A\,\mu M^{-1}\,cm^{-2}$)	Limit of detection (μM)	Characterisation techniques	Average number of graphene layers	Ref.
Acetaminophen	GC	Polydopamine functionalized rGO with Pd nanoparticles	Commercially obtained GO	5.842[a]	0.087	EDS, FTIR, SEM UV–vis and XRD	–	[43]
Acetaminophen	GC	rGO, PDDA, gold nanoparticles and alumina	Modified Hummers	4.871[a]	0.006	AFM, FT-IR, SEM, TEM and XRD	Single layer	[44]
AFP	GC	AuNPs-PEDOT/PB-rGO	–	–	0.003	SEM, TEM and XPS	–	[26]
Cd(II) and Pb(II)	GC	rGO with electrodeposited gold nanoparticles	Modified Hummers with graphite pre-treatment [20]	0.0062 and 0.0013 for Cd(II) and Pb(II), respectively	7.12×10^{-4} and 5.79×10^{-4} for Cd(II) and Pb(II), respectively	EDS and SEM	–	[45]
CRP	SPE	Bio-functionalised rGO	–	–	–	SEM	–	[46]
Cu(II)	GC	Tin sulphide on rGO	Modified Hummers (hydrazine reductant)	2.410	0.02	Raman, SEM, TEM, XPS and XRD	–	[47]
Curcumin	GC	Electrochemically reduced GO	Hydrazine-stabilised Hummers [48]	0.16	0.1	Not stated	–	[49]
DNA	GC	Fe_3O_4/rGO composite	Non-specified modified Hummers method	Reported to span several orders of magnitude	Attomolar	SEM and TEM	–	[50]
Dopamine	Freestanding graphene based composite electrode	rGO, Ag nanoparticle and poly(pyronin Y) composite paper	Modified Hummers with graphite pre-treatment [20]	0.90	0.15	Raman, SEM, STM, UV–vis, XPS and XRD	Single sheet	[27]
Dopamine	GC	rGO with electropolymerised Cu/AMT	Non-specified modified Hummers method	0.049[a]	0.004	FT-IR, SEM, XPS and XRD	–	[51]
Dopamine	GC‘	rGO with manganese tetraphenylporphyrin	Non-specified modified Hummers method	2.61	0.008	EDX, NMR, SEM, UV–vis	–	[52]
Fe(III), Cd(II) and Pb(II)	GC	Calixarene/rGO	–	–	*Ca*, 2.0×10^{-5} for all targets	AFM, IR, Raman, SEM and XPS	–	[37]
Folic acid	GC	Electrochemically reduced GO and methylene blue	Unknown – references a paper that appears ambiguous in its GO production procedure [53]	0.014	0.5	SEM and TEM	Single sheet	[54]
Glucose	GO_x and Nafion processed gate electrode	Polypyrrole nanowires and rGO	Modified Hummers [48]	0.773	0.1	FT-IR and SEM	–	[55]
Glucose	GO and polyacrylic acid hydrogel	Multi-component rGO-based electrode	Traditional Hummers [21]	0.015	25.0	FT-IR and UV–vis	–	[56]
Glucose	GC	N-doped rGO with copper nanostructures	Modified Hummers with graphite pre-treatment [20]	1.85	0.014	EDX, Raman, SEM, XRD and XPS	Few layers	[57]
Glucose	GC	Layer-by-layer assembly of rGO and glucose oxidase films	Modified Hummers with graphite pre-treatment [20]	2.47	13.4	FT-IR, SPR and XRD	“Multiple layers”	[58]
Glucose	ZnO-nanorods/graphene heterostructure	Glucose oxidase, ZnO and chemically reduced graphene on SiO_2	–	0.088	–	FT-IR, SEM, TEM and XRD	–	[33]
Glucose	GC	rGO, chitosan, ZnO, silver nanparticles, glucose oxidase	Microwave-assisted synthesis based on Hummers [59]	6.41[a]	10.6	Raman, SEM, TEM and XRD	–	[30]
Glucose	GC	rGO, Nafion®, chitosan, and glucose oxidase	Unknown – references a paper that appears ambiguous in its GO production procedure [53]	0.042	5.0	FT-IR, SEM, TEM and XPS	“Multiple layers”	[60]
Hydrogen peroxide	GC	Pd/TNM@rGO	Modified Hummers	3.678	0.0025	EELS, Raman, TEM, XPS and XRD	–	[61]
Hydrogen peroxide	Au	CeO_2/rGO	Non-specified modified Hummers method	–	0.26	FESEM, FTIR and XRD	–	[62]
Hydrogen peroxide	GC	rGO with iron nanoparticles using an ion exchange method	Traditional Hummers [21]	0.065	0.056	EDX, FTIR, TEM and XPS	Few layers	[63]
Hydrogen peroxide	GC	rGO electrodeposited upon GC with methylene blue	Modified Hummers method [64]	10.2	0.06	SEM, TEM, FT-IR and UV–vis	Single layer	[65]

Hydrogen peroxide	SPE	rGO and CeO_2	Modified Hummers method [66]	0.046	0.21	Raman, SEM, FT-IR and XRD	Multiple layers	[67]
Hydrogen peroxide	GO paper	Gold and Prussian blue nanoparticles grafted onto rGO paper	Hummers with graphite pre-treatment [20]	5.000	0.1	AFM, EDS, SEM, TEM, UV–vis XPS	Single layer	[68]
Hydrogen peroxide and Nitrite	GC	MWCNTs@rGONRs	Longitudinal unzipping of MWCNT	0.616 and 0.643 for H_2O_2 and NO_2, respectively	0.001 and 0.01 for H_2O_2 and NO_2, respectively	EDS, Raman, SEM and TEM	–	[69]
Hydroquinone	GC	rGO with chitosan	Traditional Hummers	16.8	0.44	AFM, FT-IR, EDS, SEM and XRD	–	[70]
Imatinib	PGE	Dendrimer assisted rGO	–	0.199 and 0.816	0.007	SEM	–	[71]
Lobetyolin	GC	Magnetic (Fe_3O_4) functionalised rGO	Modified Hummers with graphite pre-treatment [20]	1.91	0.043	AFM, FT-IR, TGA, and VSM, (vibrating sample magnetometer) SEM and XRD	Single sheet	[72]
Methlymercury	GC	AuNPs-rGO	Commercially obtained	0.57 ($\mu A\,\mu L^{-1}$)	0.12	EDS, Raman and SEM	–	[73]
Methylparaben	GC	rGO/RuNPs	Modified Hummers [74]	–	0.24	HPLC, Raman and TEM	–	[75]
NADH	GC	Au-AgNP,P(L-Cys)/ERGO	Electrochemical reduction	4.872	0.009	SEM and XPS	–	[31]
Nitrite	GC	pD/Fe_3O_4/polyDOPA/rGO	Commercially obtained		0.5	Raman, TEM, UV–vis, XPS and XRD	–	[76]
Nitrite	GC	3D-mp-rGO-POM	GO prepared *via* graphite oxidation and exfoliation [77]. rGO prepared *via* hydrazine reduction [78].		0.2			[79]
Nitrite	AU SPE	Screen-printed gold electrode with drop-casted rGO	Traditional Hummers	0.21	0.83	AFM, Raman, SEM	–	[80]
Nitrite	GC	Hydrothermally synthesized nitrogen-doped GO with palladium nanocubes (drop casted)	Modified Hummers with graphite pre-treatment [20]	0.342	0.11	EDS, SEM, Raman, UV–vis TEM, XRD	Few-layer	[81]
Nitrite	GC	Layer-by-layer drop-casted rGO, horseradish peroxidase, and Co_3O_4	Modified Hummers with graphite pre-treatment [20]	4.20[a]	0.21	FE-SEM, FE-SEM, UV–vis and XRD	–	[82]
Nitrite	GC	rGO with Zn-porphyrin fullerene	Commercially obtained	0.23	N/A	SEM and UV–vis	–	[83]
Nitromethane	BFE	Electrochemically reduced GO, chitosan, and haemoglobin	Commercially obtained	–	1.5	SEM	–	[84]
Ochratoxin A	BFE	DNA-functionalised graphene/Au hybrids with CdTe quantum dots	Modified Hummers with graphite pre-treatment [20]	–	0.07 pg mL^{-1}	Fluorescence spectra FS, TEM	–	[85]
Pb(II)	GC	Co_3O_4/rGO/chitosan	Commercially obtained	–	3.5×10^{-4}	EDS, SEM, TEM and XRD	–	[86]
Sulfite	GC	AuNPs-rGO	–	0.103	0.045	SEM, TEM, XRD and XPS	"Thin"	[87]
Taxifolin	GC	Poly(diallyldimethylammonium chloride) rGO and Pd nanoparticles	Traditional Hummers [21]	38.4	0.001	UV–vis TEM, XRD	–	[88]
Thyroxine	Graphene-based filler hybrid-nanomaterial throughout an insulating epoxy resin	rGO with gold nanoparticles and beta-cyclodextrin	Modified Hummers (ascorbic acid reductant)	35.5	0.001	EDS, TEM, TGA and UV–vis	–	[28]

[a] Value not stated within the paper but estimated from presented data, –; information not stated within the paper, 3D; three dimensional, mp; macroporous, AFP; α-fetoprotein, AuNPs-PEDOT/PB-rGO; gold nanoparticles-poly(3,4-ethylenedioxythiophene)/Prussian blue-reduced graphene oxide nanocomposite, BFE; bismuth coated glassy carbon, CRP; C-reactive protein, Cu/AMT; opper-2-amino-5-mercapto-1,3,4-thiadiazole, DNA; deoxyribose nucleic acid, DOPA; 3,4-dihydroxy-l-phenylalanine, EDS; energy-dispersive X-ray spectroscopy, EELS; electron energy loss spectroscopy, ERGO; electrochemically reduced graphene oxide, FESEM; field emission scanning electron microscope, FS; Fluorescense spectra, FT-IR; Fourier transform infrared spectroscopy, GC; glassy carbon electrode, GO; graphene oxide, HPLC; high performance liquid chromography, MWCNTs@rGONRs; multiwalled carbon nanotubes@reduced graphene oxide nanoribbons/chitosan, NMR; nuclear magnetic resonance, NP; nanoparticle, P(L-Cys); poly(L-Cysteine), PGE; pencil graphite electrode, POM; polyoxometalate, rGO; reduced graphene oxide, SEM; scanning electron microscope, SPE, screen-printed electrode, SPR; Surface Plasmon Resonance, STM; scanning tunnel microscope, TEM, transmission electron microscope, TGA; thermogravimetric analysis, TNM; tert-nonyl mercaptan, UV–vis; ultraviolet–visible spectroscopy, VSM; vibrating sample magnetometer, XPS; X-ray photoelectron spectroscopy, XRD; X-ray diffraction analysis.

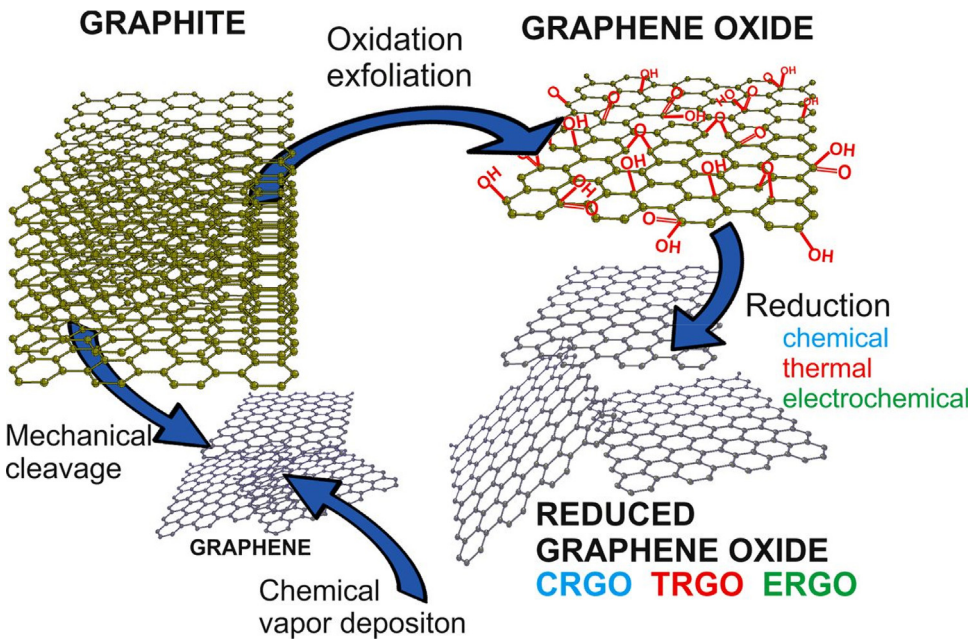

Fig. 2. A schematic illustration of possible ways for preparation of graphene and rGO.
Reproduced from Ref. [42].

Table 1 is grouped into analytical targets, the supporting electrode substrate, fabrication method, analytical outputs and characterisation techniques and number of graphene layers reported for each sensor/composite. We provide a critical summary and suggest future directions for this field.

2. GO utilised in electrochemical sensing applications

Table 1 lists selected literature over the period 2016–2017 describing electroanalytical sensors reported in the academic literature which utilise rGO in one form or another. As noted in Table 1, many of the graphene production methods rely upon solvent-based synthesis of reduced graphene oxide (rGO), which can be created by one of a number of production methods and are sometimes not reported in sufficient detail [19–21]. Each method yields rGO of different qualities, and therefore producing differing electrochemical responses that have to be accounted for. To quote one example, one recent report highlights a voltammetric determination method for the anti-inflammatory drug furazolidone [22], but the methods employ commercially available GO with an unknown production method, adding a layer of ambiguity to the work that requires removal using a range of characterization techniques, discussed previously. This is demonstrated succinctly in the work by Poh et al. that shows rGO synthesized from Staudenmaier, Hoffman, and Hummers methods yield significantly different electrochemical responses [23]. This is due to the different reagents used for the oxidation of graphite, which not only introduce different levels of oxygenated species, but also introduce impurities, especially in the case of the Hummers method, which is purported to introduce N heteroatoms to the graphene backbone. Note other reports have contradicted this [24]. It is interesting to note that the O/C ratio of Hummers-type GO has been demonstrated to vary insignificantly with respect to reagent concentrations and conditions, however the crudely-termed “oxygen-related bonds” may be more informative as to how reaction conditions in the Hummers method affects the GO structures, and hence the electrochemistry [24]. It is found from such work that controlling the residence time of the chemical reactions at 35 °C in the Hummers method has a significant effect upon the total number of oxygen bonds in the GO product. Despite this, Hummers methods are the most common due to the relative safety of the chemical reaction, as it does not use explosive chemicals. Aside from the variable oxygenated species, there is also a question of the impurities in Hummers-type rGO, often in the form of manganese (IV) structures as reported elsewhere [25]. While such materials can be beneficial, one must be aware of the level of impurity and take this into account when designing rGO-based sensors. It is clear from inspection of Table 1 that characterisation methods are not consistently applied nor are the number of layers of the material which limits comparison of the electroanalytical sensors and their fundamental understanding.

Interesting work utilising rGO have reported a gold nanoparticles-poly(3,4-ethylenedioxythiophene)/Prussian blue-reduced graphene oxide (AuNPs-PEDOT/PB-rGO) nanocomposite which has been utilised as a stable and sensitive label-free electrochemical immunosensor for detecting α-fetoprotein (AFP) [26]; see Fig. 3 for an overview of the electroanalytical platform. The use of the rGO was reported to increase the sensors performance through an increased surface area and being a useful supporting material for the Prussian blue compound. This rGO based immunosensor showed a sensitive response to AFP in a linear range from 0.01 to 50 ng mL^{-1} with a low detection limit of 3.3 pg mL^{-1} and was shown to allow the determination of AFP within human serum. Another approach for rGO fabrication is chemically reduced rGO. One recent success of this technique was reported by Kiranşan et al., who utilized HI to chemically reduce wet-synthesized graphene oxide using the method reported by Kovtyukhova et al. [20,27]. Their work describes graphene paper, fabricated using a sonicated suspension rGO, Ag nanoparticles, and pyronin Y. The mixture was transferred to a polycarbonate membrane and vacuum filtered, leaving a paper-like structure behind consisting of a rGO/AgNP/pyronin Y composite. After treatment with HI and electropolymerisation of pyronin Y using voltammetry, the paper electrode was ready to use. The electrode was employed towards dopamine detection, finding a similar performance to several other graphene composites studied previously. However, the novelty of graphene paper allows this sensor to stand out, especially since it would be feasible to scale this up into larger sheets that could be easily shaped and sized by hand. Graphene

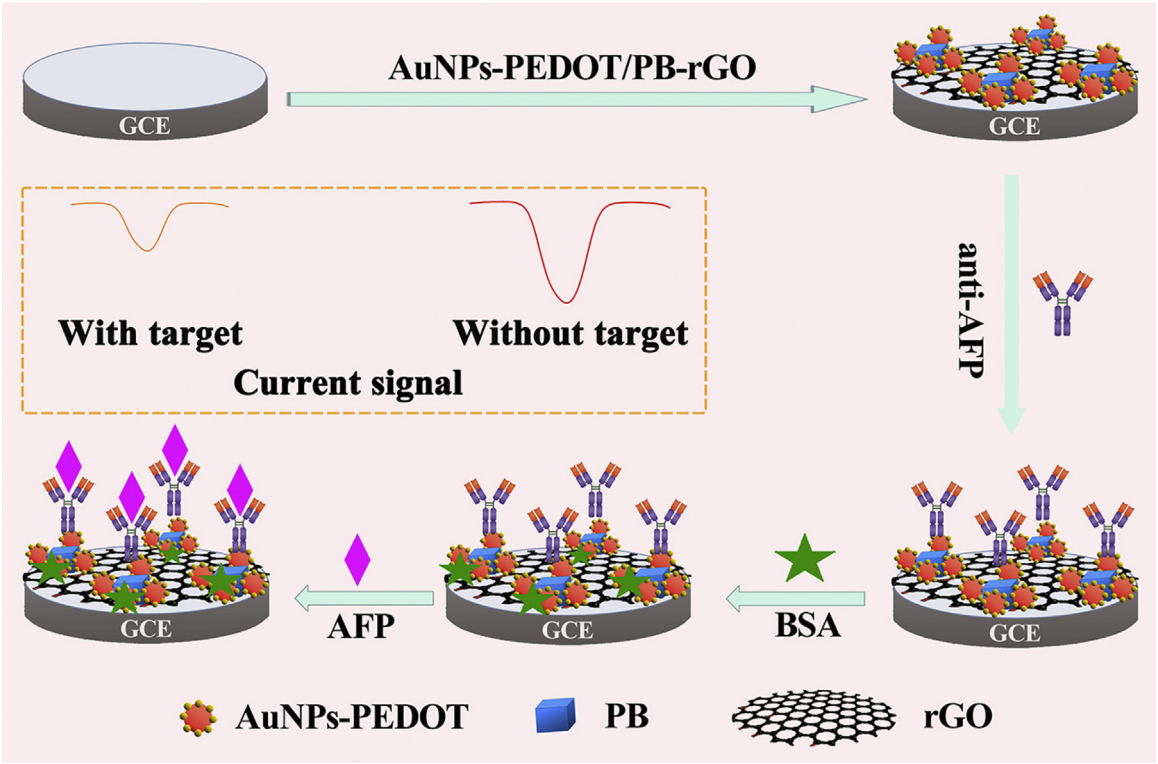

Fig. 3. Schematic diagram for the preparation of the electrochemical immunosensor.
Reproduced from Ref. [26].

paper was also reported by Zhang et al., using gold nanoparticles and Prussian blue to successfully detection hydrogen peroxide non-enzymatically to a sensitivity of 5 $\mu A\,\mu M^{-1}\,cm^{-2}$.

GO can also be incorporated into epoxy resin electrodes, carrying the advantage of long term electrode stability, durability, and repeatability over proof-of-concept approaches such as drop-casting. Muñoz et al. performed amperometric experiments using rGO made through a Hummers method with ascorbic acid as the reductant [28]. The electrode utilised gold nanoparticles and beta-cyclodextrin (see Fig. 4), which is a molecule often used in host–guest chemistry as an acceptor site for some simple biomolecules, including thyroxine. The epoxy resin approach was demonstrated to detect nanomolar concentrations of thyroxine, which are required for adequate diagnosis of thyroid activity in adults. Host–guest interactions are also exploited for the detection of BrO_3^- in water samples by Palanisamy et al. [29]. Their work exploits the host–guest properties of beta-cyclodextrin to immobilise haemoglobin upon rGO. The haemoglobin in this instance is the signal reporting aspect of the electrode due to its specificity towards the BrO_3 ion, which reduces to Br(V) to Br^-, resulting from haemoglobin's affinity for dioxygen. Microwave-assisted synthesis of graphene is the preferred approach in the work by Li et al. [30] In what is essentially a Hummers-type GO, the microwave assistance speeds up the fabrication process for the rGO. The rGO is then subjected to further microwave treatment in the presence of $Ag(NO_3)_2$ and $Zn(CH_3CH_2COO)_2$ in the presence of ethanol and NaOH to create a platform for glucose oxidase to attach efficiently. The approach reports lower detection limits than similar works, though the linear ranges are notably smaller.

Electrochemically reduced graphene oxide (ERGO) has been used as the basis of an ethanol biosensor where nicotinamide adenine dinucleotide (NADH) is used as a mediator with gold-silver bimetallic nanoparticles (Au-AgNPs), poly(L-Cysteine) (P(L-Cys)) immobilised upon the ERGO [31]. Fig. 5 provides a summary of the various steps required to produce the sensor. This composite electrode is reported to exhibit an excellent electrocatalytic response towards NADH at a low oxidation potential (+0.35 V) and minimization of surface contamination due to the synergistic effects of the Au-AgNPs, polymer and ERGO [31]. This ERGO based sensor was also used as a sensitive ethanol biosensor, which was prepared with alcohol dehydrogenase (ADH) via glutaraldehyde, bovin serum albumin and nafion (Naf). There was a linear response for ethanol in the concentration range from 0.017 to 1.845 mM with a low detection limit of 5.0 μM reported. The GCE/Au-AgNPs/P(L-Cys)-ERGO/ADH/Naf based sensor was utilised as the basis of an ethanol sensor in different commercial beverages (Fig. 6).

Other notable works include the detection of dopamine by Kim et al., who utilised chemically cleaned rGO on a glassy carbon electrode as the working electrode in their work [32]. In many respects, their work demonstrates that simplicity can be a good thing in electroanalytical sensing devices, because they only use the two elements in their electrode design. Such electrodes may not exhibit the selectivity characteristics that an enzymatic system may offer, but for the case of dopamine detection, this is not an issue provided the electrochemical oxidation peaks of dopamine, ascorbic acid, and uric acid can be independently discerned. Their work observes dopamine the presence of 1 mM ascorbic acid with a sensitivity of 0.588 $\mu A\,\mu M^{-1}\,cm^{-2}$. The limit of detection was estimated to be 2.64 μM, which is around the average level of dopamine passed in urine by an adult in the western world.

Other methods use rGO as a growth substrate for heterostructures of metal oxides. One such example is the work by Zhao et al., who grew ZnO nanorods on rGO that are used as molecular wires [33]. Their work uses a rGO thin film prepared by filtering rGO suspensions through a membrane, collecting the rGO upon the membrane. The rGO was dried and transferred to a SiO_2 substrate, then ZnO was hydrothermally grown at 90 °C for 1 h. The approach is fairly simple in its nature and provides a more robust

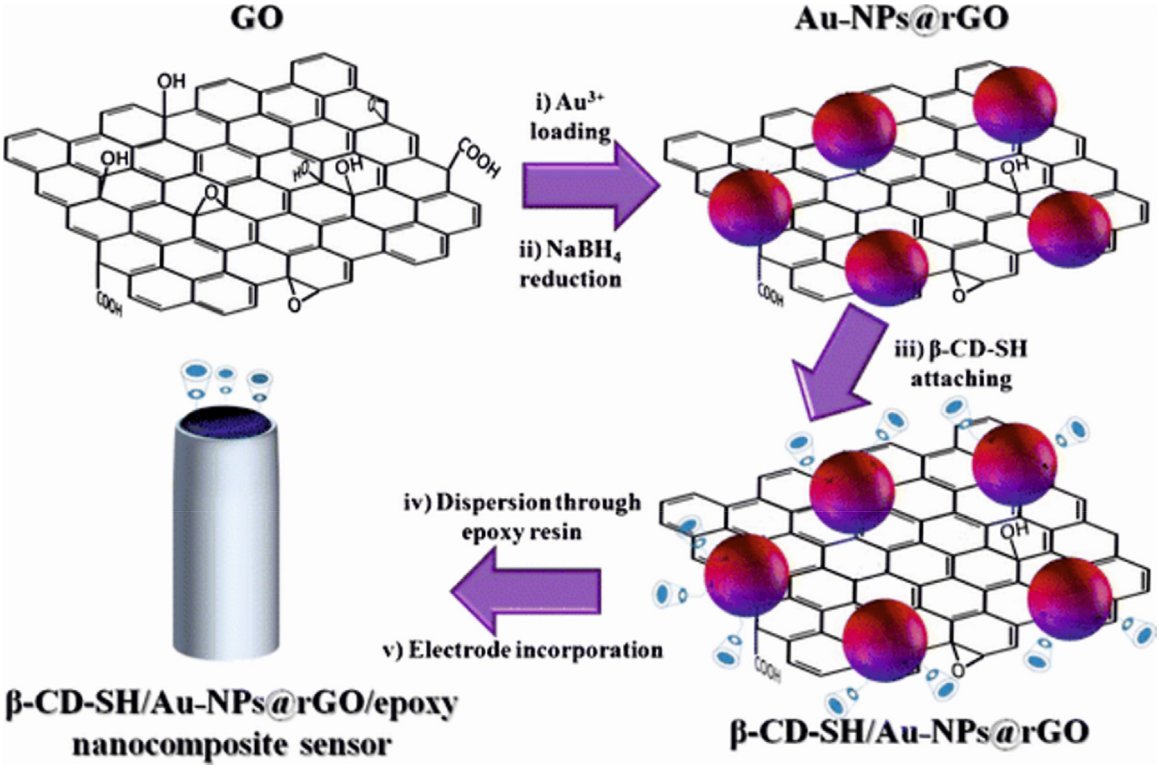

Fig. 4. Synthetic route of Au-NP@rGO and β-CD-SH/Au-NP@rGO hybrid-materials from GO and their subsequently dispersion in epoxy resin for nanocomposite sensor purposes.
Reproduced from Ref. [28].

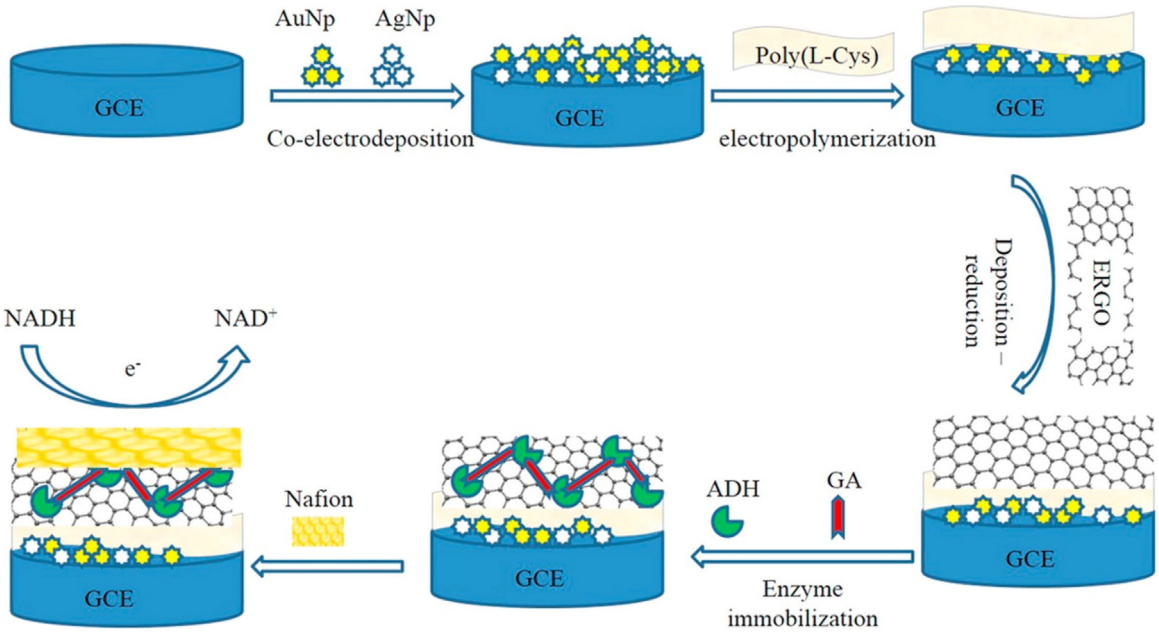

Fig. 5. Schematic illustration of the stepwise ethanol biosensor fabrication process.
Reproduced from Ref. [31].

method for a repeatable graphene-based electrode. The electrode was used to anchor glucose oxidase, providing a centre for glucose oxidation that could be efficiently transmitted to the potentiostat through the synergistic effect of the rGO network and the ZnO molecular wires transferring the signal from glucose oxidase. The sensor was demonstrated to have a sensitivity to glucose of 17.64 μA mM^{-1}, which is comparable to similar methods in the current literature (see Table 1). Electrochemically reduced graphene oxide (ERGO) films have been utilised to modify screen-printed electrodes (SPE) for the detection of Zn/Cd and Pd [34], and pencil graphite electrodes for the detection of Pd in milk Samples [35]. In both cases the detection mechanism was *via* stripping

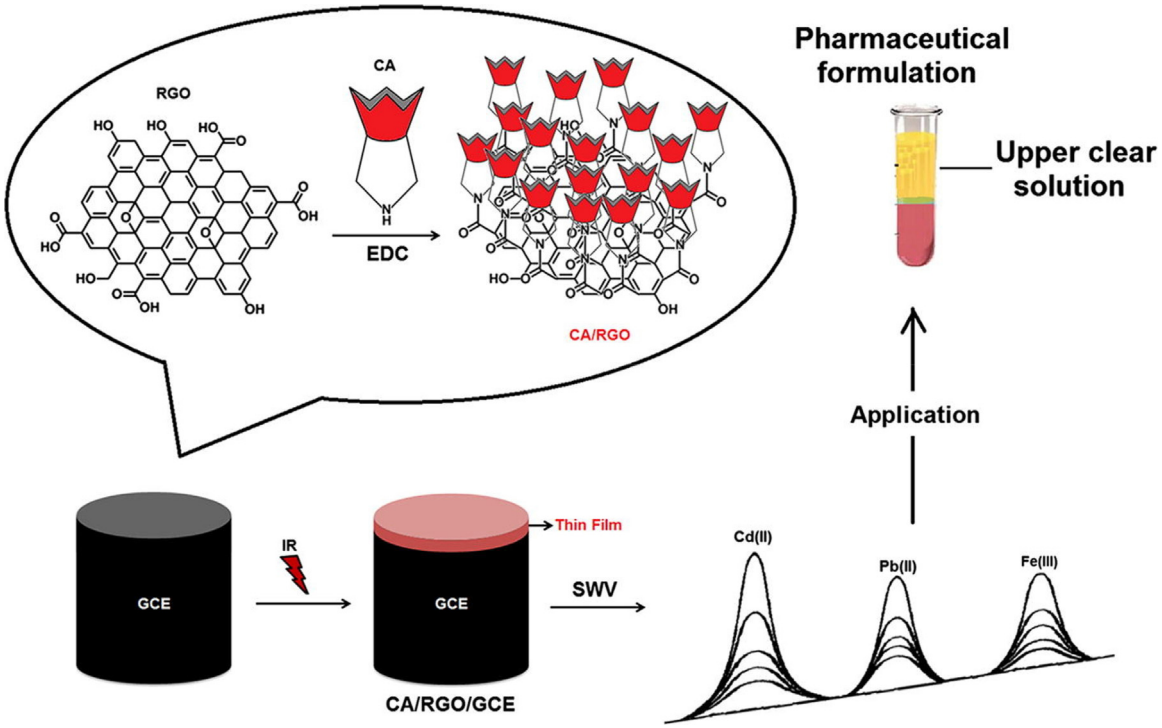

Fig. 6. Preparation of CA/RGO/GCE and nano-sensing of the guest metal ions.
Figure reproduced from Ref. [37].

voltammetry. Improvements in sensor performance was observed using rGO, adsorbed onto large surface area electrodes, giving rise to favourable electron transfer sites.

The summary of the use of rGO as the basis of the sensor is that it is mainly used to increase the assessable electrochemically active area and also provide stability for the immobilisation of electrocatalytic compounds/moieties. In the case that the electrochemical mechanism is diffusionally based, the peak current is governed by the Randles-Ševćik equation [36], and the increase in the electrochemically active area, where the electroanalytical sensor is based upon rGO (rather than say a compound modified upon its surface), will give rise to larger voltammetric currents and hence a larger signal output which should improve the sensitivity and limit of detection. However, control experiments using just graphite (or similar) are not routinely performed and needs to be undertaken in cases where rGO is reported to give rise to significant outputs. One area that benefits greatly from the use of rGO is where the underlying electrochemical mechanism is adsorption based, as is the case *via* stripping voltammetry, where the increased surface area gives rise to a greater proportion of adsorption sites and hence improvements in the sensors performance will be realised. This has been reported, for example by Göde et al. [37] modified a glassy carbon electrode (GCE) with calixarene functionalized reduced graphene oxide (CA/RGO) and applied it to the sensing of, Fe(II), Cd(II) and Pb(II), in aqueous solutions. The CA/RGO was found to significantly improve the sensitivity of electrochemical responses and separation of the target heavy metals. The electrochemical oxidation of Fe(III), Cd(II), and Pb(II) was performed by square wave voltammetry (SWV) with analytically useful detection limits possible with the sensor applied into pharmaceutical formulations [37]. Clearly such approaches, have merit capitalising upon the underlying electrochemical mechanism, *i.e.* adsorptive over diffusional which really shows the benefit of using rGO.

3. Concluding remarks

This review has explored the recent field of using rGO as the basis of electroanalytical sensors, where mainly it is found that rGO is the basis of sensor and is usually modified with nanoparticles or electrocatalytic moieties. In this approach, rGO is reported to provide a larger surface area and stable surface onto which nanoparticles and electrocatalytic compounds are reproducibility immobilised. However, in other cases there are no justifications of why rGO is beneficial or why it is being used when graphite could equally be usefully utilised. The large surface area of rGO is beneficially utilised when the electrochemical mechanism is adsorptive in nature, this is exemplified when used in stripping voltammetry. Our analysis of the field suggests the following is addressed in future publications, which are currently seldom considered:

- Consider the amount of rGO used in sensors and consider coverage experiments to determine the optimal amount of rGO required.
- The number of layers of rGO should be reported to allow direct comparison and reproducibility in the field.
- Since rGO is not fully reduced, *i.e.* to pristine graphene, the C/O ratio, amount and C—O groups/types needs to be deduced as these might contribute to the electrochemical response.
- Controls are made with graphite for the proposition of rGO as in most instances, based on the design of the sensor, the former is more than adequate.
- The methodology of the rGO fabrication is made, i.e. following the work of Pumera et al. [38] which overviews the terminology that should be incorporated, *i.e.* chemically rGO should be notated as CrGO or similar to allow future understanding and differentiation.
- The underlying supporting electrode material is not usually explored and this will have an effect upon the electrochemical

sensor due to the supporting electrodes roughness and rGO-electrode substrate interactions. Generally however, if a sensor is really going to be implemented into the field, the research should be undertaken upon screen-printed electrodes which allow translation of research from the laboratory in-to-the field due their scales of economy and high reproducibility [39,40].

References

[1] K.S. Novoselov, D. Jiang, F. Schedin, T.J. Booth, V.V. Khotkevich, S.V. Morozov, A.K. Geim, Proc. Natl. Acad. Sci. USA 102 (2005) 10451–10453.
[2] K.S. Novoselov, A.K. Geim, S.V. Morozov, D. Jiang, Y. Zhang, S.V. Dubonos, I.V. Grigorieva, A.A. Firsov, Science 306 (2004) 666–669.
[3] D.A.C. Brownson, D.K. Kampouris, C.E. Banks, Chem. Soc. Rev. 41 (2012) 6944–6976.
[4] D.R. Dreyer, S. Park, C.W. Bielawski, R.S. Ruoff, Chem. Soc. Rev. 39 (2010) 228–240.
[5] C. Schafheut, J. Prakt, Chemistry 21 (1840) 129–157.
[6] B.C. Brodie, Philos. Trans. R. Soc. Lond. 149 (1859) 249–259.
[7] S.H. Dave, C. Gong, A.W. Robertson, J.H. Warner, J.C. Grossman, ACS Nano 10 (2016) 7515–7522.
[8] A. Ambrosi, A. Bonanni, Z. Sofer, J.S. Cross, M. Pumera, Chem. Eur. J. 17 (2011) 10763–10770.
[9] A. Bonanni, A. Ambrosi, M. Pumera, Chem. Eur. J. 18 (2012) 4541–4548.
[10] M.A. Pope, C. Punckt, I.A. Aksay, J. Phys. Chem. C 115 (2011) 20326–20334.
[11] M. Muti, S. Sharma, A. Erdem, P. Papakonstantinou, Electroanalysis 23 (2011) 272–279.
[12] D.A.C. Brownson, G.C. Smith, C.E. Banks, R. Soc. Open Sci. 4 (2017).
[13] M. Velický, D.F. Bradley, A.J. Cooper, E.W. Hill, I.A. Kinloch, A. Mishchenko, K.S. Novoselo, H.V. Patten, P.S. Toth, A.T. Valota, S.D. Worrall, R.A.W. Dryfe, ACS Nano 8 (2014) 10089–10100.
[14] W. Yuan, Y. Zhou, Y. Li, C. Li, H. Peng, J. Zhang, Z. Liu, L. Dai, G. Shi, Sci Rep. 3 (2013) 2248.
[15] A.G. Güell, N. Ebejer, M.E. Snowden, J.V. Macpherson, P.R. Unwin, J. Am. Chem. Soc. 134 (2012) 7258–7261.
[16] A.G. Güell, A.S. Cuharuc, Y.-R. Kim, G. Zhang, S.-y. Tan, N. Ebejer, P.R. Unwin, ACS Nano 9 (2015) 3558–3571.
[17] D.A.C. Brownson, S.A. Varey, F. Hussain, S.J. Haigh, C.E. Banks, Nanoscale 6 (2014) 1607–1621.
[18] E.P. Randviir, D.A.C. Brownson, C.E. Banks, Mater. Today 17 (2014) 426–432.
[19] J. Chen, B. Yao, C. Li, G. Shi, Carbon 64 (2013) 225–229.
[20] N.L. Kovtyukhova, P.J. Ollivier, B.R. Martin, T.E. Mallouk, S.A. Chizhik, E.V. Buzaneva, A.D. Gorchinskiy, Chem. Mater. 11 (1999) 771–778.
[21] W.S. Hummers, R.E. Offeman, J. Am. Chem. Soc. 80 (1958) 1339.
[22] S. Shahrokhian, L. Naderi, M. Ghalkhani, Mater. Sci. Eng. C 61 (2016) 842–850.
[23] H.L. Poh, F. Sanek, A. Ambrosi, G. Zhao, Z. Sofer, M. Pumera, Nanoscale 4 (2012) 3515–3522.
[24] J. Guerrero-Contreras, F. Caballero-Briones, Mater. Chem. Phys. 153 (2015) 209–220.
[25] C.H.A. Wong, Z. Sofer, M. Kubešová, J. Kučera, S. Matějková, M. Pumera, Proc. Natl. Acad. Sci. USA 111 (2014) 13774–13779.
[26] T. Yang, H. Jia, Z. Liu, X. Qiu, Y. Gao, J. Xu, L. Lu, Y. Yu, J. Electroanal. Chem. 799 (2017) 625–633.
[27] K.D. Kıranşan, E. Topçu, M. Alanyalıoğlu, J. Appl. Polym. Sci. 134 (2017) 45139.
[28] J. Muñoz, M. Riba-Moliner, L.J. Brennan, Y.K. Gun'ko, F. Céspedes, A. González-Campo, M. Baeza, Microchim. Acta 183 (2016) 1579–1589.
[29] S. Palanisamy, Y.-T. Wang, S.-M. Chen, B. Thirumalraj, B.-S. Lou, Microchim. Acta 183 (2016) 1953–1961.
[30] Z. Li, L. Sheng, A. Meng, C. Xie, K. Zhao, Microchim. Acta 183 (2016) 1625–1632.
[31] G.A. Tığ, Talanta 175 (2017) 382–389.
[32] Y.-R. Kim, S. Bong, Y.-J. Kang, Y. Yang, R.K. Mahajan, J.S. Kim, H. Kim, Biosens. Bioelectron. 25 (2010) 2366–2369.
[33] Y. Zhao, W. Li, L. Pan, D. Zhai, Y. Wang, L. Li, W. Cheng, W. Yin, X. Wang, J.-B. Xu, Y. Shi, Sci. Rep. 6 (2016) 32327.
[34] K. Pokpas, S. Zbeda, N. Jahed, N. Mohamed, P.G. Baker, Int. J. Electrochem. Sci. 9 (2014) 736–759.
[35] J. Ping, Y. Wang, J. Wu, Y. Ying, Food Chem. 151 (2014) 65–71.
[36] R.G. Compton, C.E. Banks, Understanding Voltammetry, Imperial College Press, London, 2011.
[37] C. Göde, M.L. Yola, A. Yılmaz, N. Atar, S. Wang, J. Colloid Interface Sci. 508 (2017) 525–531.
[38] M. Pumera, Electrochem. Commun. 36 (2013) 14–18.
[39] C.W. Foster, R.O. Kadara, C.E. Banks, Screen-Printing Electrochemical Architectures, Springer International Publishing, Germany, 2016.
[40] D.A.C. Brownson, C.E. Banks, The Handbook of Graphene Electrochemistry, Springer, London, 2014.
[41] R. Raccichini, A. Varzi, S. Passerini, B. Scrosati, Nat. Mater. 14 (2015) 271–279.
[42] J. Filip, J. Tkac, Electrochim. Acta 136 (2014) 340–354.
[43] L. Fu, G. Lai, D. Zhu, B. Jia, F. Malherbe, A. Yu, ChemCatChem 8 (2016) 2975–2980.
[44] J. Li, W. Sun, X. Wang, H. Duan, Y. Wang, Y. Sun, C. Ding, C. Luo, Anal. Bioanal. Chem. 408 (2016) 5567–5576.
[45] G. Zhao, H. Wang, G. Liu, Z. Wang, J. Cheng, Ionics 23 (2017) 767–777.
[46] R.S. Singal, R.K. Kotnala, Appl. Biochem. Biotechnol. 183 (2017) 672–683.
[47] J. Lu, X. Zhang, N. Liu, X. Zhang, Z. Yu, T. Duan, J. Electroanal. Chem. 769 (2016) 21–27.
[48] D. Li, M.B. Muller, S. Gilje, R.B. Kaner, G.B. Wallace, Nat. Nano 3 (2008) 101–105.
[49] D. Zhang, X. Ouyang, J. Ma, L. Li, Y. Zhang, Electroanalysis 28 (2016) 749–756.
[50] H. Teymourian, A. Salimi, S. Khezrian, Electroanalysis 29 (2017) 409–414.
[51] Y. Li, Y. Gu, B. Zheng, L. Luo, C. Li, X. Yan, T. Zhang, N. Lu, Z. Zhang, Talanta 162 (2017) 80–89.
[52] S. Sakthinathan, H.F. Lee, S.-M. Chen, P. Tamizhdurai, J. Colloid Interface Sci. 468 (2016) 120–127.
[53] C. Su, M. Acik, K. Takai, J. Lu, S.-J. Hao, Y. Zheng, P. Wu, Q. Bao, T. Enoki, Y.J. Chabal, K.P. Ping, C. Su, M. Acik, K. Takai, J. Lu, S.-J. Hao, Y. Zheng, P. Wu, Q. Bao, T. Enoki, Y.J. Chabal, K.P. Ping, Nat. Commun. 3 (2012) 1298.
[54] D. Zhang, X. Ouyang, W. Ma, L. Li, Y. Zhang, Electroanalysis 28 (2016) 312–319.
[55] Y. Wang, X. Qing, Q. Zhou, Y. Zhang, Q. Liu, K. Liu, W. Wang, M. Li, Z. Lu, Y. Chen, D. Wang, Biosens. Bioelectron. 95 (2017) 138–145.
[56] H. Al-Sagur, S. Komathi, M.A. Khan, A.G. Gurek, A. Hassan, Biosens. Bioelectron. 92 (2017) 638–645.
[57] N.S.K. Gowthaman, A.M. Raj, S.A. John, ACS Sustain. Chem. Eng. 5 (2017) 1648–1658.
[58] D.B.T. Mascagni, C.M. Miyazaki, N.C.D. Cruz, M.L.D. Moraes, A. Riul, M. Ferreira, Mater. Sci. Eng. C 68 (2016) 739–745.
[59] Z. Li, C. Xie, J. Wang, A. Meng, F. Zhang, Sens. Actuators B 208 (2015) 505–511.
[60] A. Rabti, W. Argoubi, N. Raouafi, Microchim. Acta 183 (2016) 1227–1233.
[61] S. Bozkurt, B. Tosun, B. Sen, S. Akocak, A. Savk, M.F. Ebeoğlugil, F. Sen, Anal. Chim. Acta 989 (2017) 88–94.
[62] X. Yang, Y. Ouyang, F. Wu, Y. Hu, Y. Ji, Z. Wu, Sens. Actuators B 238 (2017) 40–47.
[63] B. Amanulla, S. Palanisamy, S.-M. Chen, V. Velusamy, T.-W. Chiu, T.-W. Chen, S.K. Ramaraj, J. Colloid Interface Sci. 487 (2017) 370–377.
[64] S. Stankovich, R.D. Piner, X. Chen, N. Wu, S.T. Nguyen, R.S. Ruoff, J. Mater. Chem. 16 (2006) 155–158.
[65] D. Zhang, X. Ouyang, L. Li, B. Dai, Y. Zhang, J. Electroanal. Chem. 780 (2016) 60–67.
[66] Y. Xu, H. Bai, G. Lu, C. Li, G. Shi, J. Am. Chem. Soc. 130 (2008) 5856–5857.
[67] Z. Yao, X. Yang, F. Wu, W. Wu, F. Wu, Microchim. Acta 183 (2016) 2799–2806.
[68] M. Zhang, A. Halder, C. Hou, J. Ulstrup, Q. Chi, Bioelectrochemistry 109 (2016) 87–94.
[69] V. Mani, M. Govindasamy, S.-M. Chen, T.-W. Chen, A.S. Kumar, S.-T. Huang, Sci. Rep. 7 (2017) 11910.
[70] Y. Yang, Q. Wang, W. Qiu, H. Guo, F. Gao, J. Phys. Chem. C 120 (2016) 9794–9803.
[71] B. Hatamluyi, Z. Es'haghi, J. Electroanal. Chem. 801 (2017) 439–449.
[72] B. Sun, X. Gou, R. Bai, A.A.A. Abdelmoaty, Y. Ma, X. Zheng, F. Hu, Mater. Sci. Eng. C 74 (2017) 515–524.
[73] Y. Xu, W. Zhang, J. Shi, X. Zou, Y. Li, E.T. Haroon, X. Huang, Z. Li, X. Zhai, X. Hu, Food Chem. 237 (2017) 423–430.
[74] F.H. Cincotto, T.C. Canevari, S.A.S. Machado, A. Sánchez, M.A.R. Barrio, R. Villalonga, J.M. Pingarrón, Electrochim. Acta 174 (2015) 332–339.
[75] C.D. Mendonça, T.M. Prado, F.H. Cincotto, R.T. Verbinnen, S.A.S. Machado, Sens. Actuators B 251 (2017) 739–745.
[76] Z. Zhao, Z. Xia, C. Liu, H. Huang, W. Ye, Electrochim. Acta 256 (2017) 146–154.
[77] D.C. Marcano, D.V. Kosynkin, J.M. Berlin, A. Sinitskii, Z. Sun, A. Slesarev, L.B. Alemany, W. Lu, J.M. Tour, ACS Nano 4 (2010) 4806–4814.
[78] Y. Kim, S. Shanmugam, ACS Appl. Mater. Interfaces 5 (2013) 12197–12204.
[79] G. Ma, M. Yang, F. Xu, L. Wang, Anal. Methods 9 (2017) 5140–5148.
[80] A. Gholizadeh, D. Voiry, C. Weisel, A. Gow, R. Laumbach, H. Kipen, M. Chhowalla, M. Javanmard, Microsyst. Nanoeng. 3 (2017) 17022.
[81] Y. Shen, D. Rao, W. Bai, Q. Sheng, J. Zheng, Talanta 165 (2017) 304–312.
[82] H. Liu, K. Guo, J. Lv, Y. Gao, C. Duan, L. Deng, Z. Zhu, Sens. Actuators B 238 (2017) 249–256.
[83] S. Fan, J. Yang, T. Wei, J. Zhang, N. Zhang, M. Chai, X. Jin, H. Wu, Talanta 160 (2016) 713–720.
[84] Y. Wen, W. Wei, X. Zhang, S. Wang, Biosens. Bioelectron. 79 (2016) 894–900.
[85] N. Hao, L. Jiang, J. Qian, K. Wang, J. Electroanal. Chem. 781 (2016) 332–338.
[86] Y. Zuo, J. Xu, F. Jiang, X. Duan, L. Lu, H. Xing, T. Yang, Y. Zhang, G. Ye, Y. Yu, J. Electroanal. Chem. 801 (2017) 146–152.
[87] H. Yu, X. Feng, X.-X. Chen, S.-S. Wang, J. Jin, J. Electroanal. Chem. 801 (2017) 488–495.
[88] Q. Wang, L. Wang, G. Li, B. Ye, Talanta 164 (2017) 323–329.